2061/12/9

Framework of probabilistic and deterministic methods for evaluating near-fault displacement

Inoue, N. (GRI) , Tonagi, M., Takahama, T., Matsumoto, Y.(KKE) , Kitada, N. (GRI) , Dalguer, Luis A. (Swiss Nuc.) and Irikura, K. (Aichi Univ.)

Project Framework

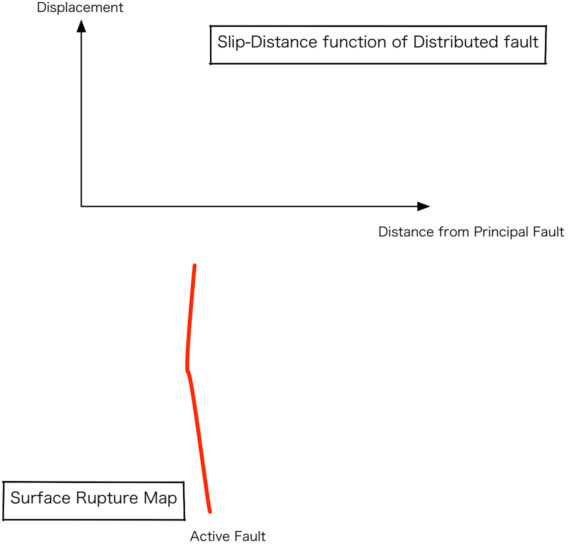

In Japan, the important facilities can not be constructed on the active faults.

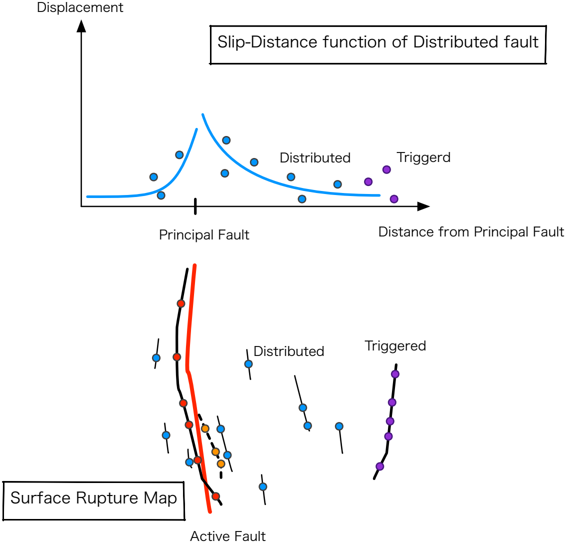

After the earthquake. . . .

The evaluation of distributed fault displacement is more important.

Project Framework

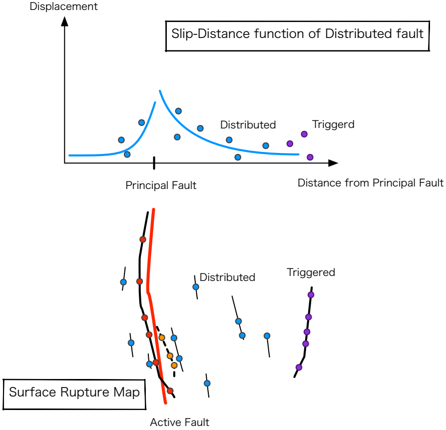

Probabilistic Approach (Empirical Method)

Project Framework

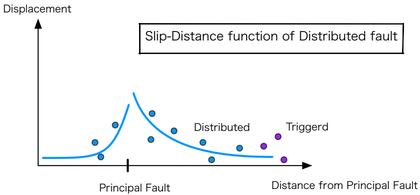

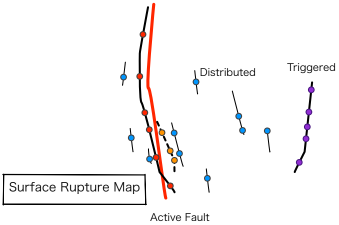

Probabilistic Approach (Empirical Method)

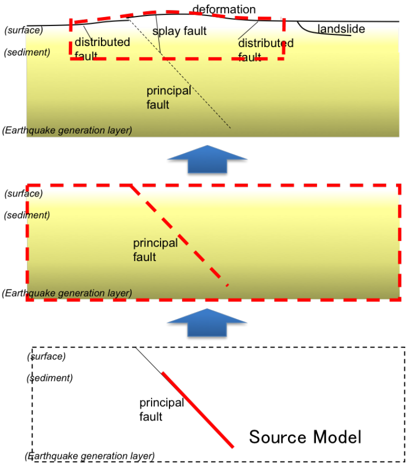

Deterministic Approach (Theoretical Method)

Evaluation method for fault displacement by deterministic Method

(3) Simulation of subsurface rupture considering terrain, stratum structure and non-linear.

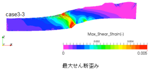

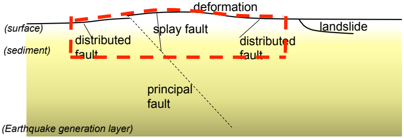

(2) Reproduction of earthquake motion with period of 10 seconds or more by Dynamic rupture simulation.

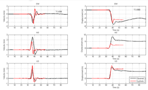

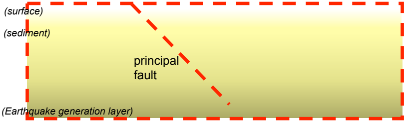

(1) Characterized source model that can be reproduced up to 10 seconds in period.

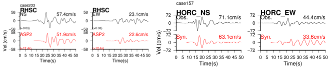

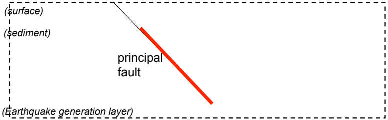

- ✓ We try to explain observed motion with a simple fault geometry.
- ✓ We set initial source model referring to slip distribution obtained by Sekiguchi and Iwata (2001).
- ✓ Referring to characterized source model by Kamae and Irikura (2002) and Ikeda et al. (2004), we tune up parameters of strong ground motion areas (SMGAs) by trial and error, such as size, location, rake angle and rise time to simulate observed velocity ground motions well.

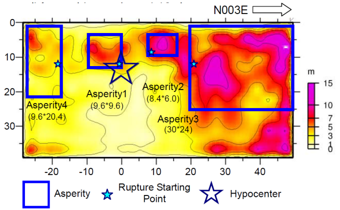

Ikeda et al. (2004)

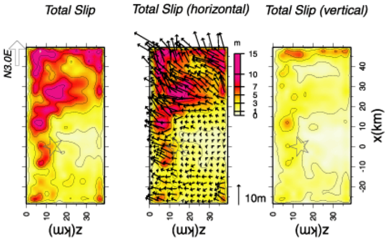

Sekiguchi and Iwata (2001)

Target : 2.0 – 10 s

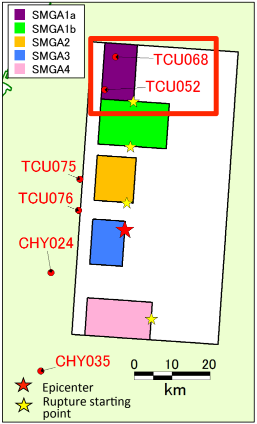

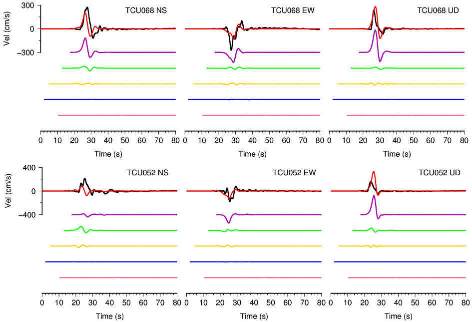

— Obs. — Syn. (all SMGAs) — Syn. (SMGA1a) — Syn. (SMGA1b) — Syn. (SMGA2) — Syn. (SMGA3) — Syn. (SMGA4)

Target : 2.0 – 10 s

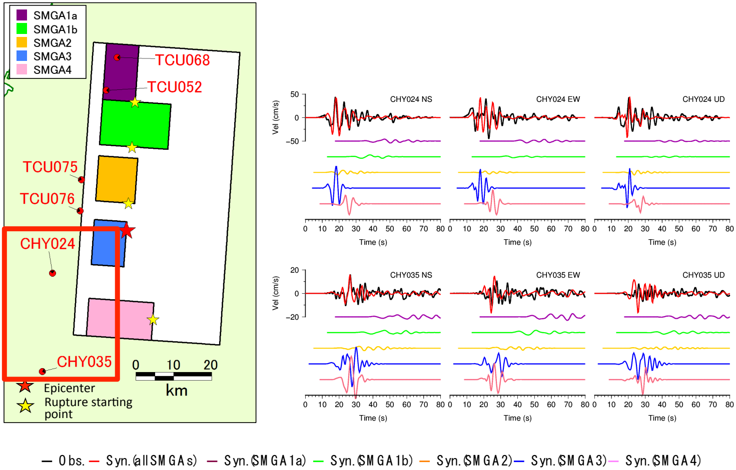

Target : 2.0 – 10 s

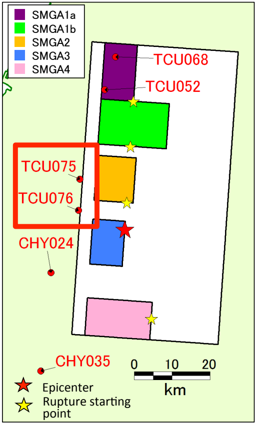

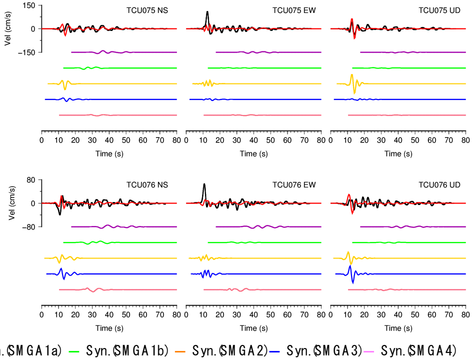

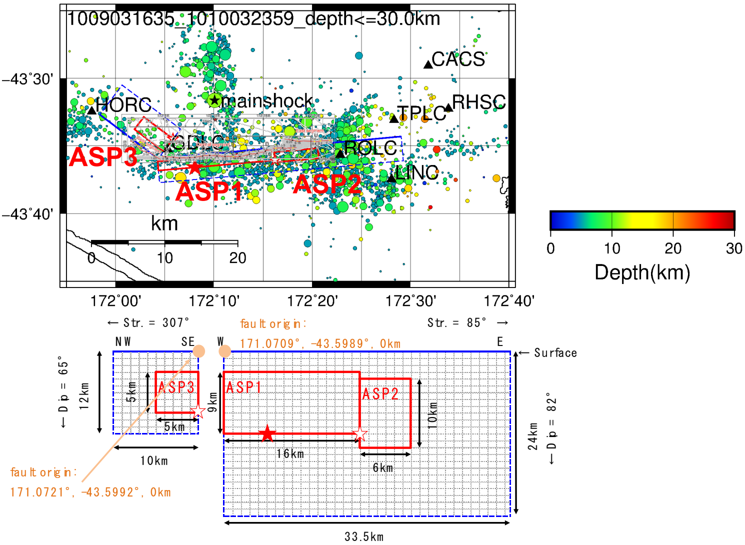
1009031635_1010032359_depth<=30.0km
CACS
RHSC
TPLC
HORC
mainshock
GDLC
ROLC
LINC
ASP3
ASP1
ASP2
km
0
10
20
−43˚30'
−43˚40'
172˚00'
172˚10'
172˚20'
172˚30'
172˚40'
0
10
20
30
Depth(km)
← Str. = 307°
fault origin:
171.0709°, -43.5989°, 0km
Str. = 85° →
NW
SE
W
E
← Surface
← Dip = 65°
12km
5km
ASP3
5km
10km
9km
ASP1
ASP2
10km
16km
6km
24km
← Dip = 82°
33.5km
fault origin:
171.0721°, -43.5992°, 0km

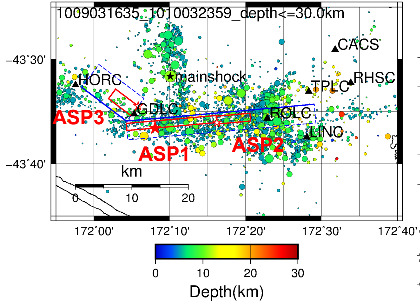
1009031635_1010032359_depth<=30.0km
CACS
HORC
mainshock
TPLC
RHSC
GDLC
ROLC
LINC
ASP3
ASP1
ASP2
km
0
10
20
-43°30'
-43°40'
172°00'
172°10'
172°20'
172°30'
172°40'
Depth(km)
0
10
20
30

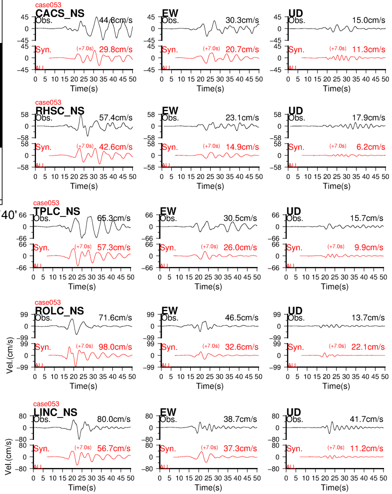
case053
CACS_NS Obs. 44.8cm/s Syn. 29.8cm/s
EW Obs. 30.3cm/s Syn. 20.7cm/s
UD Obs. 15.0cm/s Syn. 11.3cm/s
RHSC_NS Obs. 57.4cm/s Syn. 42.6cm/s
EW Obs. 23.1cm/s Syn. 14.9cm/s
UD Obs. 17.9cm/s Syn. 6.2cm/s
TPLC_NS Obs. 65.3cm/s Syn. 57.3cm/s
EW Obs. 30.5cm/s Syn. 26.0cm/s
UD Obs. 15.7cm/s Syn. 9.9cm/s
ROLC_NS Obs. 71.6cm/s Syn. 98.0cm/s
EW Obs. 46.5cm/s Syn. 32.6cm/s
UD Obs. 13.7cm/s Syn. 22.1cm/s
LINC_NS Obs. 80.0cm/s Syn. 56.7cm/s
EW Obs. 38.7cm/s Syn. 37.3cm/s
UD Obs. 41.7cm/s Syn. 11.2cm/s
(+7.0s)
Time(s)
Vel.(cm/s)

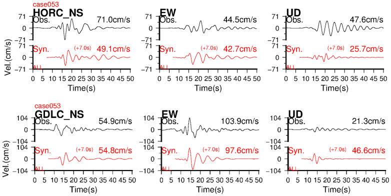
case053
HORC_NS Obs. 71.0cm/s Syn. 49.1cm/s
EW Obs. 44.5cm/s Syn. 42.7cm/s
UD Obs. 47.6cm/s Syn. 25.7cm/s
GDLC_NS Obs. 54.9cm/s Syn. 54.8cm/s
EW Obs. 103.9cm/s Syn. 97.6cm/s
UD Obs. 21.3cm/s Syn. 46.6cm/s
(+7.0s)
Time(s)
Vel.(cm/s)

Characterized Source Model: ChiChi

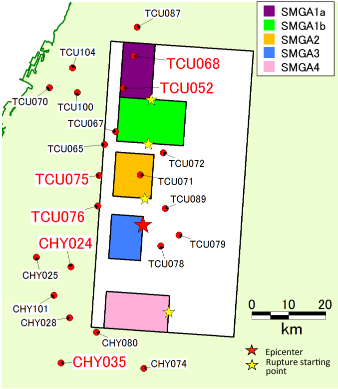

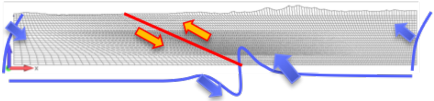

Numerical Simulation: ChiChi

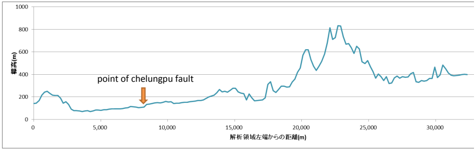

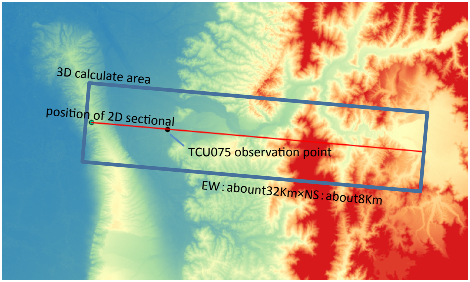

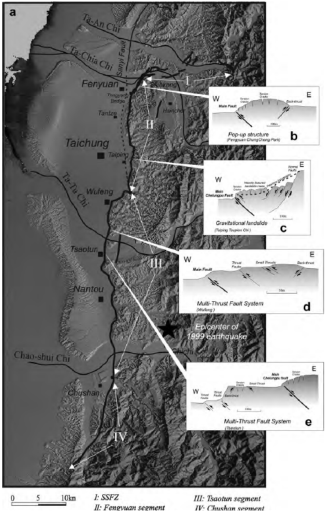

Numerical Simulation: ChiChi

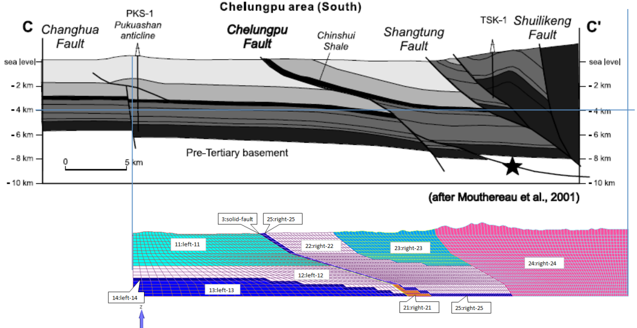

Fig 7 Model of Underground structure and computational mesh

Table 4 ground property

Material ID		S-wave Velocity(m/s)	density (Kg/m³)	Poisson's ratio	Shearing rigidity (N/m²)
11, 23		1,550	2,000	0.3	4.81e+9
12, 22		1,700	2,050	0.3	5.92e+9
14, 25		1,550	2,000	0.3	4.81e+9
13		2,500	2,300	0.3	1.44e+10
21		2,500	2,300	0.3	1.44e+10
24		2,500	2,300	0.3	1.44e+10

Table 5 property of fault plane (Joint element)

Young's mod(N/m²)	Poisson's ratio	cohesion (N/m²)	ϕ (°)
7.0e+9	0.33	3.92e+4	1

Table 6 Judge of failure (Drucker-Prager type)

cohesion (N/m²)	ϕ (°)	ratio of after failure
1.50e+6	30	0.01

【Linear Analysis】

【Consider elastic-plastic model of ground】

x-displacement

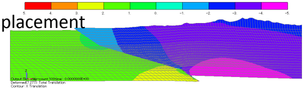

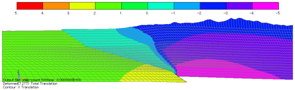

z-displacement

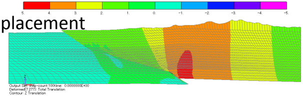

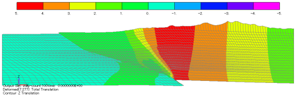

shear strain

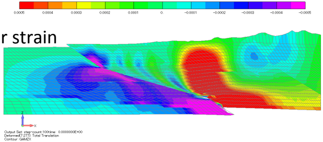

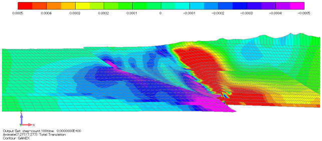

Table 7 Comparative list of displacement

		observation	Linear Analysis of ground	elastic-plastic model
X-disp	hanging	-1.5～-4m	-1.33m	-0.12m
	footwall	0.97m	1.07m	1.20m
Z-disp	hanging	2～4m	1.61m	0.80m
	footwall	-0.15m	-0.12m	-0.14m

region of failure(red)

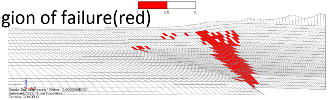

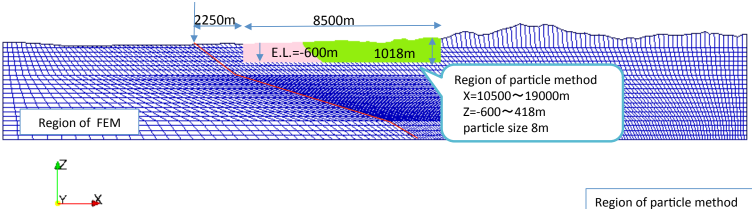

Table 3 ground property

	density [kg/m³]	Young's modulus [Pa]	Poisson's ratio	cohesion [Pa]	ϕ
mat1	2050	5.925E+09	0.30	1.5E+6	30.0
mat2	2000	4.805E+09	0.30	1.5E+6	30.0

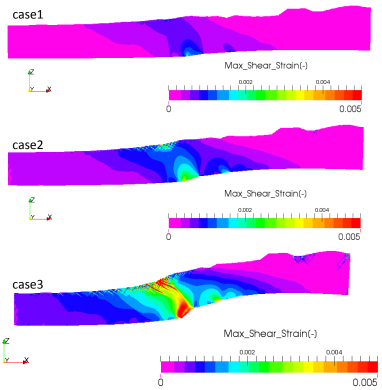

Max Shear Strain

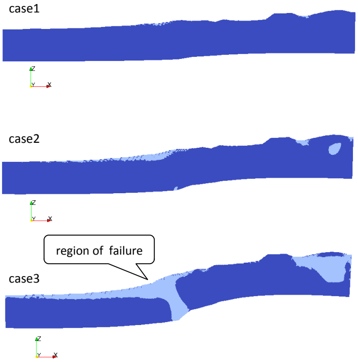

region of failure

Event	Type	Mw	Refarence
2014Nagano	R	6.2	Okada et al. (2015)
2008IwateMiyagi	R	6.9	TODA et al. (2010)
1995Kobe	S	6.9	AWATA and Mizuno (1998)
1945Mikawa	R	6.7	Sugito and Okada (2004)
1943Tottori	S	7.0	Kaneda and Okada (2002)
1930Kita Izu	S	6.9	MATSUDA (1972)
1927Kita Tango	S	7.1	OKADA and MATSUDA (1997)
1896Rikuu	R	6.7	Matsuda et al. (1981)
1891Nobi	S	7.4	MATSUDA (1974)
2005Kashmir	R	7.6	Kaneda et al. (2008)
1999ChiChi	R	7.4	Azuma et al. (2000)
1971San Fernando	R	6.7	Kamb et al. (1971); U.S. Geological Survey (1971)
1986Marryat	R	5.9(Ms)	Bowman and Barlow (1991)

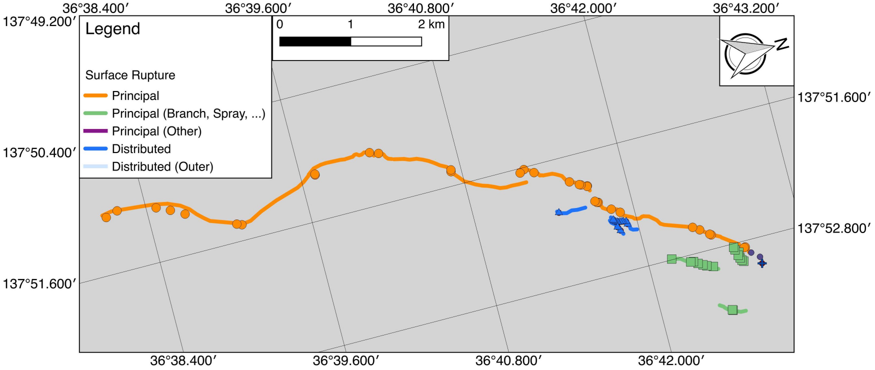
36°38.400′
36°39.600′
36°40.800′
36°42.000′
36°43.200′
137°49.200′
137°50.400′
137°51.600′
137°52.800′
Legend
Surface Rupture
Principal
Principal (Branch, Spray, ...)
Principal (Other)
Distributed
Distributed (Outer)
0
1
2 km
N

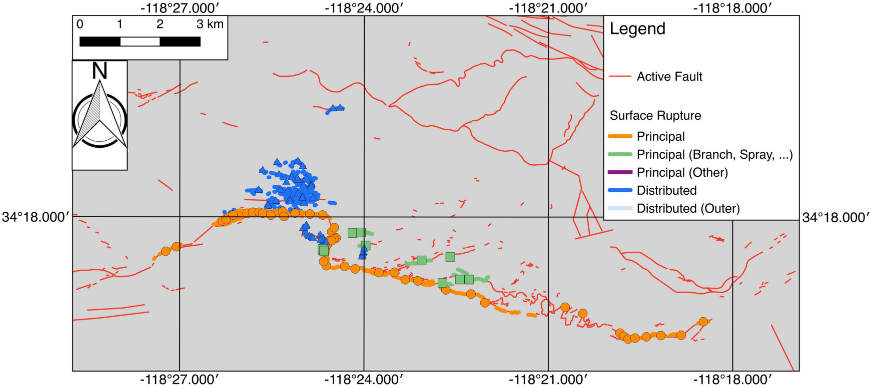
-118°27.000′
-118°24.000′
-118°21.000′
-118°18.000′
0 1 2 3 km
N
34°18.000′
34°18.000′
Legend
Active Fault
Surface Rupture
Principal
Principal (Branch, Spray, ...)
Principal (Other)
Distributed
Distributed (Outer)
-118°27.000′
-118°24.000′
-118°21.000′
-118°18.000′

Principal Fault Slip-Distance Relation (Strike-Slip)

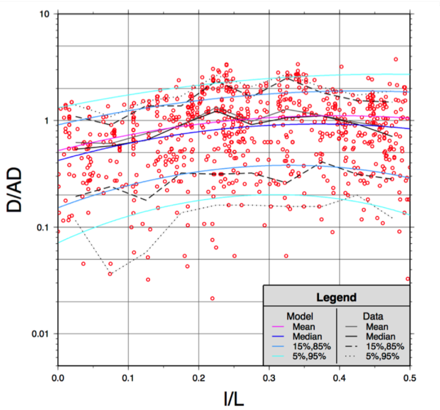

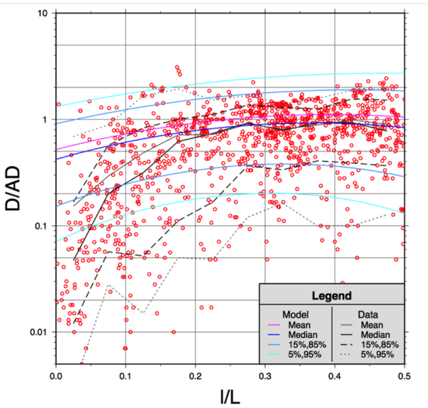

Principal Fault Slip-Distance Relation (Reverse-Slip)

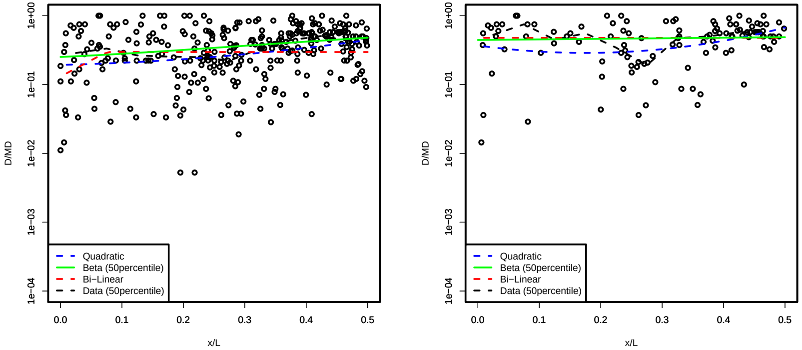

Distributed (Reverse-Slip)

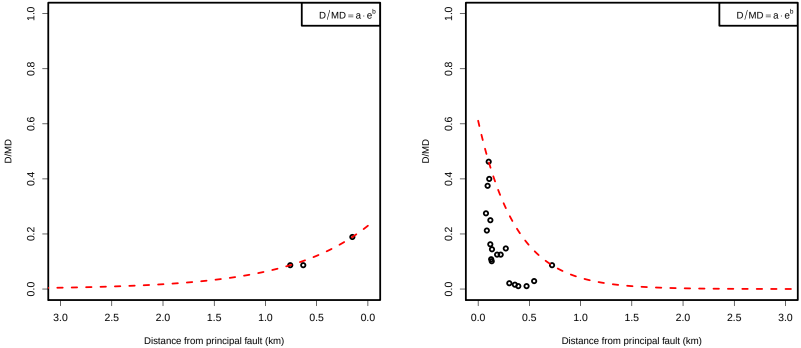

Distributed (Strike-Slip)

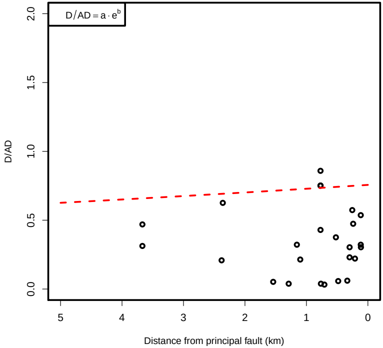

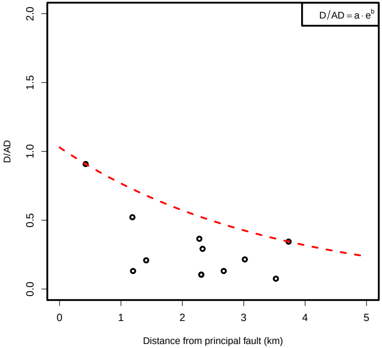

Distributed (Strike-Slip)

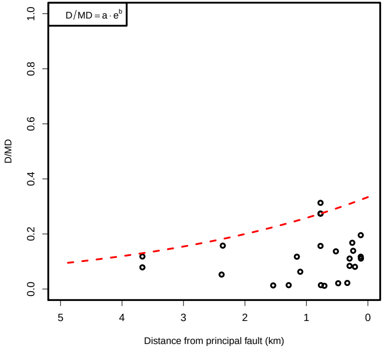

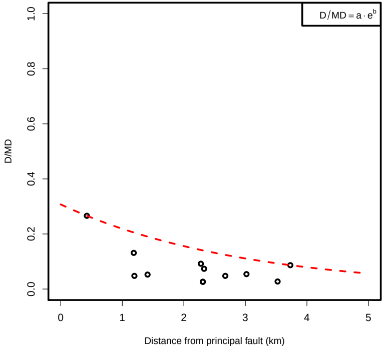

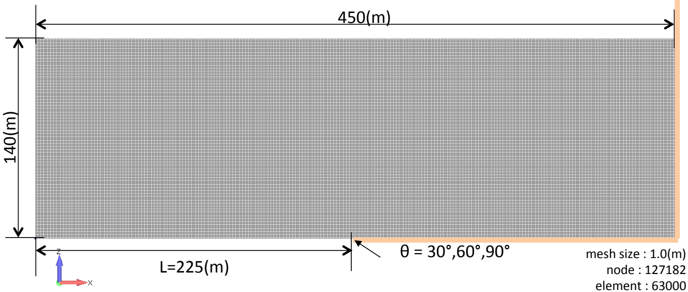

mesh size : 1.0(m)
node : 127182
element : 63000

Table 1 ground property

Material	density (Kg/m³)	Poisson's ratio	Shearing rigidity (N/m²)
1	2,000	0.3	4.80e+9

Table 2 Judge of failure (Drucker-Prager type)

cohesion (N/m²)	ϕ (°)
1.50e+6	8

Numerical Simulation Parametric Study

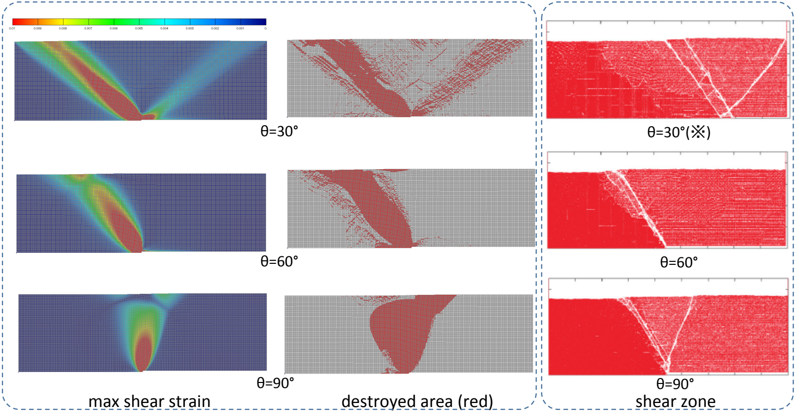

FEM(This study) DEM

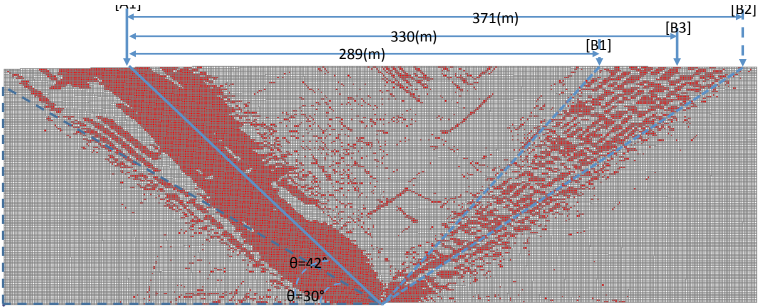
[A1]
371(m)
[B2]
[B3]
330(m)
[B1]
289(m)
θ=42°
θ=30°

Concluding Remarks

We introduced the our framework to evaluate near-fault displacement based on deterministic and probabilistic approaches.

We introduced the our framework to evaluate near-fault displacement based on deterministic and probabilistic approaches.

■ Deterministic Approach
· Characterized Source Model: reproduce the observed waveforms
· Surface Displacement Simulation: the results depend on the boundary condition and material property.

We introduced the our framework to evaluate near-fault displacement based on deterministic and probabilistic approaches.

■ Deterministic Approach
・Characterized Source Model: reproduce the observed waveforms
・Surface Displacement Simulation: the results depend on the boundary condition and material property.

■ Probabilistic Approach
・Displacement data is limited, especially for distributed fault

We introduced the our framework to evaluate near-fault displacement based on deterministic and probabilistic approaches.

■ Deterministic Approach
・Characterized Source Model: reproduce the observed waveforms
・Surface Displacement Simulation: the results depend on the boundary condition and material property.

■ Probabilistic Approach
・Displacement data is limited, especially for distributed fault

■ For better understanding of fault displacement
・Comparison and combination of both approachs

Thank you for your kind attention

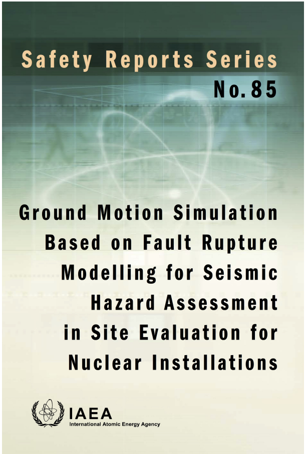

3.4.6. Response spectrum for design and analysis. 40
3.4.7. Selection of near fault time histories for design and analysis 40
3.4.8. Scaling and matching of near fault time histories 41
3.4.9. Orientation of components 42

4. EXAMPLES OF GROUND MOTION EVALUATION BASED ON HETEROGENEOUS SOURCE MODELS. 42

4.1. Examples of predicted ground motions based on the SMGA/asperity model. 42
4.1.1. Crustal earthquake 42
4.1.2. Subduction interface earthquake 44
4.1.3. Intra-slab earthquake 47
4.2. Examples of ground motion evaluation based on the hybrid method 49
4.3. Uncertainty in ground motion prediction using fault rupture modelling 54
4.4. Examples of uncertainty treatment 57

5. CONCLUSIONS 59

5.1. Advantages and disadvantages of different approaches 59
5.2. Roles of ground motion simulations and GMPEs 60

APPENDIX I: ESTIMATION OF FAULT PARAMETERS FOR THE SMGA/ASPERITY MODEL. 61

APPENDIX II: OPEN ACCESS TO THE SCEC BROADBAND SIMULATION PLATFORM 79

REFERENCES 81

ANNEX: FAULT DISPLACEMENT HAZARD ANALYSIS 93

CONTRIBUTORS TO DRAFTING AND REVIEW 125

Related publication from IAEA

[1] Okada, Shinsuke, Ishimura, Daisuke, Niwa, Yuichi, and Toda, Shinji (2015) 「The First Surface . Rupturing Earthquake in 20 Years on a HERP Active Fault is Not Characteristic: The 2014 Mw 6.2 Nagano Event along the Northern Itoigawa–Shizuoka Tectonic Line」, *Seismological Research Letters*, 第 86 巻, 第 5 号, 1287-1300 頁.

[2] TODA, Shinji, MARUYAMA, Tadashi, YOSHIMI, Masayuki, KANEDA, Heitaro, AWATA, Yasuo, YOSHIDA, Toshikazu, and ANDO, Ryosuke (2010) "Surface Rupture Associated with the 2008 Iwate-Miyagi Nairiku, Japan, Earthquake and its Implications to the Rupture Process and Evaluation of Active Faults," *Zisin (Journal of the Seismological Society of Japan. 2nd ser.)*, Vol. 62, No. 4, pp. 153–178.

[3] AWATA, Yasuo and Mizuno, Kiyohide (1998) "Explanatory text of the strip map of the surface fault ruptures associated with the 1995 Hyogo-Ken Nanbu Earthquake, central Japan - the Nojima, Ogura and Nadagawa Earthquake Fault, scale 1:10000," *Tectonic map series*, Vol. 12, No. 1, p. 74.

[4] Sugito, Nobuhiko and Okada, Atsumasa (2004) "Surface rupture associated with the 1945 Mikawa earthquake," *Active Fault Research*, Vol. 24, pp. 103-127.

[5] Kaneda, Heitaro and Okada, Atsumasa (2002) "Surface rupture associated with the 1943 Tottori earthquake," *Active Fault Research*, Vol. 21, pp. 73-91.

[6] MATSUDA, Tokihiko (1972) *Surface faults associated with Kita-Izu earthquake of 1930 in Izu Peninsula, Japan*, Tokai University Press, 73–93 頁.

[7] OKADA, Atsumasa and MATSUDA, Tokihiko (1997) "Surface faults associated with the Kita-Tango Earthquake of 1927 in the northwestern part of Kinki district, central Japan.," *Active Fault Research*, Vol. 16, pp. 95–135.

[8] Matsuda, Tokihiko, Yamazaki, Haruo, Nakata, Takashi, and Imaizumi, Toshifumi (1981) "The surface Faults Assoicated with the Rikuu Earthquake of 1896," *Bulletin of the Earthquake Research Institute, University of Tokyo*, Vol. 55, No. 2, pp. 795–855.